International Journal of Electrical and Computer Engineering (IJECE)
Vol. 14, No. 5, October 2024, pp. 4879~4887
ISSN: 2088-8708, DOI: 10.11591/ijece.v14i5.pp4879-4887

Rotor angle deviation regulator to enhance the rotor angle stability of synchronous generators

Nor Syaza Farhana Mohamad Murad[1], Muhammad Nizam Kamarudin[1], Muhammad Iqbal Zakaria[2]
[1]Center for Robotics and Industrial Automation (CeRIA), Faculty of Electrical Technology and Engineering, Universiti Teknikal Malaysia Melaka, Melaka, Malaysia
[2]School of Electrical Engineering, College of Engineering, Universiti Teknologi MARA, Selangor, Malaysia

Article Info

Article history:

Received Jan 10, 2024
Revised Jun 20, 2024
Accepted Jul 2, 2024

Keywords:

Lyapunov
Nonlinear swing equation
Power system
Rotor angle stability
Synchronous generator

ABSTRACT

Occurrences of disturbance affect the rotor angle operation of a synchronous generator in the generation system of a power system. The disturbance will disrupt the synchronous generator's rotor oscillation and result in rotor angle instability, which will degrade the power system's performance. This paper aims to develop a Lyapunov-based rotor angle deviation regulator for the nonlinear swing equation of a synchronous generator. The proposed regulator is expected to assure asymptotic stability of the rotor angle and robustness to uncertainty. Backstepping and Lyapunov redesign techniques are employed in developing the regulator. To validate the effectiveness and robustness of the regulator, a simulation in MATLAB/Simulink is carried out. The simulation result shows that the asymptotic stability and robustness of the regulator are guaranteed regardless of the disturbance.

Corresponding Author:

Muhammad Nizam Kamarudin
Center for Robotics and Industrial Automation (CeRIA), Faculty of Electrical Technology and Engineering, Universiti Teknikal Malaysia Melaka
Hang Tuah Jaya, 76100 Durian Tunggal, Melaka, Malaysia
Email: nizamkamarudin@utem.edu.my

1. INTRODUCTION

The transmission of electrical energy from the generation system to consumers is one of the most critical functions of the power system [1]. The generator ensures the stability of the power system function even in the event of a breakdown, making the generating system, in spite of the transmission and distribution systems, the most crucial part of the power system [2], [3]. The most often used generators in generating systems are synchronous generators.

The fast expansion of the human population and the rising desire for sustainability have made the electricity system's stability even more important. Maintaining the stability of the power system is essential to preventing blackouts and transmission failures, which enhances the system's overall dependability and stability. The stability of the power system is categorized into rotor angle stability, frequency stability, and voltage stability [4]. Rotor angle stability is one of the most significant forms of power system stability when it comes to synchronous generators in power systems. It focuses on the ability of generators to maintain the rotor angle when encountering disturbances [5]. Small signal stability and large signal stability are the two categories into which it may be divided. The small disturbance condition, which describes disturbances that happen slowly and randomly, is taken into account by small signal stability [6]. The capacity of the system to return to synchronism in the presence of a significant disruption is referred to as large signal stability, often called transient stability [4], [6].

The presence of disturbance will perturb the oscillation of the rotor angle of the synchronous generator, which leads to instability. The angle formed by the relative positions of the rotor axis and the resulting magnetic field axis is known as the power angle, or rotor angle. In typical operating circumstances, this angle remains constant. However, the relative motion starts when disturbances occur because the rotor will either accelerate or decelerate in relation to the synchronously rotating air gap magnetomotive force (MMF). The nonlinear differential equation, known as the swing equation, describes this relative motion [7]. The stability of the synchronous generator is preserved if the rotor locks back into synchronous speed. In the event that the disturbances do not cause a net change in power, the rotor resumes its regular operating state; if not, it works at a new power angle that corresponds to the synchronously rotating field [8]. If the rotor angle changes as a result of disturbances, the synchronous generator's performance degrades. Thus, developing a control method to increase transient performance, ensure robustness against rotor angle deviation due to disturbances, and ensure quick rotor angle regulation is critical.

Numerous publications have been published in recent years that have investigated rotor angle stability using various methodologies while emphasizing only the assessment of stability without suggesting a controller for stabilization enhancement: the Lyapunov exponent method [9], the voltage source converter-based high-voltage direct current method [10], the energy index based on the normal form method [11], the stability index vector [12], the Lyapunov direct method [7], the maximum Lyapunov exponent [13], the fault-on trajectory [14], and the probabilistic neural network [15]. These assessments focus on how quickly and accurately the analysis can be performed, which is expected to aid in power system planning by providing a protection system and corrective action, resulting in a safe power system [14], [16]. Nevertheless, several publications published in recent years have conducted research on rotor angle stability augmentation using a variety of methodologies. Charafeddine *et al.* [17] used Euler's numerical solution but neglected damping power and were constrained to small signal stability. Neglecting the damping power is an impractical assumption since it serves a crucial role in minimizing the difference between the two angular velocities [18]. Moreover, the authors employed fault clearing time, which is proven to aid in power system operation. The studies in [19], [20] employed a power system stabilizer (PSS) to regulate rotor angle stability; however, tuning the stabilizer consumed more time, and the study was confined to small signal stability only. On the other hand, sliding mode control is utilized in the enhancement of rotor angle stability by the studies [21], [22], but chattering is inevitable. Observer-based controllers are also used to improve rotor angle stability, but the dominance of the observer's linear part over the nonlinear part diminishes the impact of the nonlinear term [23]. Model predictive control is another way used to improve rotor angle stability, although the study [24] is confined to small signal stability only. Abubakar *et al.* [25] employed a resistive-type superconducting fault current limiter (R-SFCL), but fault clearing time is required to be well predetermined beforehand.

Thus, the Lyapunov-based algorithm named rotor angle deviation regulator (RADR) is proposed as the control approach in this study to ensure rotor angle stability. Despite linearizing the synchronous generator's swing equation, the proposed research utilizes a nonlinear swing equation without neglecting damping power to assure the robustness of the proposed control technique. Furthermore, the use of a nonlinear swing equation is predicted to ensure stability regardless of small and transient disturbances.

2. ROTOR ANGLE DEVIATION REGULATOR

The rotor angle deviation regulator (RADR) algorithm for a nonlinear swing equation is developed using the backstepping control technique and the robust Lyapunov redesign approach since the Lyapunov redesign is effective in dealing with uncertainty. The benefits of combining these two methodologies are guaranteeing stable control of output tracking, compensating for matched and unmatched uncertainties, and ensuring the robustness of the control algorithm [26]. In order to design the RADR via backstepping and the Lyapunov redesign technique, the state variable equation of the nonlinear swing equation is considered as in (1) and (2).

$$\dot{x_1} = x_2 \tag{1}$$

$$\dot{x_2} = -\frac{\pi f_0}{H} D x_2 + \xi + \Delta u + u \tag{2}$$

where H is the inertia constant, D denotes the damping power, u denotes the controller, ξ denotes the nonlinearity as in (3), and Δu denotes the input uncertainty as in (4).

$$\xi = -\frac{\pi f_0}{H} (P_{max} \sin \delta_0 \cos x_1 + P_s \sin x_1) \tag{3}$$

$$\Delta u = \frac{\pi f_0}{H}(\Delta P + P_m) - \frac{d^2\delta_0}{dt^2} \quad (4)$$

From (3) and (4), P_s is the synchronizing coefficient, ΔP is the fault, P_m is the mechanical power, and δ_0 is the initial rotor angle. The first step in stabilizing systems (1)–(2) is to examine its nominal system; in this study, a nominal system is defined as one that lacks the nonlinearity, ξ. Let us examine the following nominal system for (1) and (2).

$$\dot{x_1} = x_2 \quad (5)$$

$$\dot{x_2} = -\frac{\pi f_0}{H} D x_2 + \Delta u + u_{nom} \quad (6)$$

Equation (6) describes how nominal control law, u_{nom} acts as the control input for the subsystem. The primary goal of the controller is to maintain $x_1 = 0$ as t→∞ by a desired $u_{nom}(x_1)$. The design phase is limited by Lyapunov stability requirements. Algebraic manipulation of $x_2 = \phi_1(x_1) + z$ is used to subsystem (5) to increase design process flexibility. The time derivative of x_2 is therefore represented as $\dot{x_2} = \dot{\phi_1}(x_1) + \dot{z}$ and rearranges to $\dot{z} = \dot{x_2} - \dot{\phi_1}(x_1)$. The system (5) and (6) is recast as (7) and (8) when (6) is substituted for $\dot{z}$. To make the notation simpler, $\phi_1(x_1)$ is then represented as ϕ_1 onward.

$$\dot{x_1} = \phi_1 + z \quad (7)$$

$$\dot{z} = -\frac{\pi f_0}{H} D x_2 + \Delta u + u_{nom} - \dot{\phi_1} \quad (8)$$

The Lyapunov function for (7) and (8) is chosen as $V(x_1, z) = \frac{1}{2}x_1^2 + \frac{1}{2}z^2$ in order to obtain asymptotic stability. The derivative of the Lyapunov function is computed as (9).

$$\dot{V}(x_1, z) = x_1\dot{x_1} + z\dot{z}$$
$$\dot{V}(x_1, z) = x_1\phi_1 + z\left[x_1 - \frac{\pi f_0}{H} D x_2 + \Delta u + u_{nom} - \dot{\phi_1}\right] \quad (9)$$

The derivative of V must be a negative-definite function such that $\dot{V}(x_1, z) = -K_1x_1^2 - K_2z^2 \leq 0$. The solution of ϕ_1 can be found by considering the derivative of $\dot{V}(x_1)$ from (9) such that $\dot{V}(x_1) = x_1\phi_1$. From negative semi-definite function of $\dot{V}(x_1)$, which is written as $\dot{V}(x_1) \leq -K_1x_1^2$, the solution of ϕ_1 is obtained as $-K_1x_1$. Then, considering the $\dot{V}(z) \leq -K_2z^2$, the solution obtained as $-K_2z = x_1 - \frac{\pi f_0}{H} D x_2 + \Delta u + u_{nom} - \dot{\phi_1}$ and the solution of $\dot{\phi_1}$ is $-K_1x_2$. Rearranging the solution of $\dot{V}(x_1, z)$ renders (10) and (11).

$$\phi_1 = -K_1x_1 \quad (10)$$

$$-K_2z = x_1 - \frac{\pi f_0}{H} D x_2 + \Delta u + u_{nom} - \dot{\phi_1} \quad (11)$$

which is then solved and obtained u_{nom} as (12), which verified the asymptotic stability condition of the nominal control law.

$$u_{nom} = -K_2z - x_1 + \frac{\pi f_0}{H} D x_2 - \Delta u - K_1x_2 \quad (12)$$

Then, systems (1) and (2) are recalled continuing the design process. The algebraic manipulation is repeated for subsystem (1), which renders.

$$\dot{x_1} = \phi_1 + z \quad (13)$$

$$\dot{z} = -\frac{\pi f_0}{H} D x_2 + \xi + \Delta u + u - \dot{\phi_1} \quad (14)$$

The Lyapunov function is chosen as $V(x_1, z) = \frac{1}{2}x_1^2 + \frac{1}{2}z^2$, which then renders the derivative as (15).

$$\dot{V}(x_1, z) = x_1\dot{x_1} + z\dot{z}$$
$$\dot{V}(x_1, z) = x_1\phi_1 + z\left[x_1 - \frac{\pi f_0}{H} D x_2 + \xi + \Delta u + u - \dot{\phi_1}(x_1)\right] \quad (15)$$

The design is continued with a robust Lyapunov redesign technique. A robust controller is intended to assure attainable system performance for a system in the presence of nonlinearity [26]. The robust control law, u_r is designed with the help of a saturated function, as in (16).

$$u_r(x) = -\frac{\xi(x)\, n(x)}{\left(\frac{\partial V_2}{\partial x}\right)\xi(x)} \tag{16}$$

Such that

$$n(x) = \frac{\left(\left(\frac{\partial V_2}{\partial x}\right)\xi(x)\right)^2}{\left(\frac{\partial V_2}{\partial x}\right)\xi(x) + \varepsilon e^{-\alpha_1 t}}, \ \varepsilon>0, \ \alpha_1>0 \tag{17}$$

and $\xi(x)$ is observable.

The control law, u is generated by adding the nominal control law, u_{nom} and the robust control law, u_r. Thus, the control law is written as (18).

$$u = -K_2 z - x_1 + \frac{\pi f_0}{H} D x_2 - \Delta u - K_1 x_2 - \xi \frac{z\xi}{z\xi + \tau e^{-\alpha t}}, \ \varepsilon>0, \ \alpha_1>0 \tag{18}$$

Which satisfied the robust design inequality of $\dot{V}_2(z) \leq -K_1 x_1^2 - K_2 z^2 + \tau e^{-\alpha t}$.

3. RESULTS AND DISCUSSION

The experiment is conducted on a single-machine infinite-bus system. Four case studies were carried out to illustrate the RADR's efficacy in rotor angle stability. The first case study is analyzed using the stable system (system without fault), whereas the other three case studies are based on the one used in study [27], which involves three fault occurrence situations: in the middle of the transmission line ($fault = 0.63$ p.u.), at bus 1 with zero to ground impedance ($fault = 1.8$ p.u.), and at bus 1 with j 0.01 p.u. to the ground ($fault = 0.4$ p.u.), where p.u. indicates per unit. Then, the fault in cases 2, 3, and 4 was cleared by removing the faulted line after 2.5 and 6.5 cycles, which is also known as fault clearing time (FCT). The result is acquired by MATLAB simulation using the Simulink toolbox. Transient response performance is examined in the study, which includes rising time, settling time, peak time, and peak overshoot. Furthermore, the transient response's performance index in terms of integral of absolute error (IAE), integral of squared error (ISE), and sum of squared error (SSE) was examined. These evaluations are crucial for determining the efficacy and robustness of the produced RADR.

3.1. Transient response performance for all case studies

The transient response performances for each case study, both with and without RADR implemented in the system, are displayed in Figure 1. The lines on the graph are colored differently to indicate the various tested systems: the black line indicates the system without a fault, the red line indicates the system with 0.63 p.u. faults, the blue line indicates the system with 1.8 p.u. faults, and the green line indicates the system with 0.4 p.u. faults. The plotted graph indicates that different results are obtained for each tested system in the absence of RADR implementation, suggesting that the faults in the system have an effect on the rotor angle deviation of the synchronous generator. Additionally, as the dotted line in Figure 1 illustrates, the installation of fault clearing time had an impact on the synchronous generator's rotor angle deviation as well, reducing it in all faulty systems.

As illustrated in Figure 1, the application of RADR leads to minimized rotor angle deviation, which is represented as a straight line across 0°. This advocates that RADR regulates the rotor angle deviation to consistently approach 0°, thereby accomplishing the proposed objective of asymptotic rotor angle stability. The transient response performances detail is tabulated in Table 1.

Observation from Table 1 found that except for the tested system of 1.8 p.u. fault with no-fault clearing time, the transient response with RADR results in a slower rise time and settling time but enhanced performance in terms of peak undershoot and peak time. The percentage decrease in terms of settling time for the no-fault case is 170.54%, 0.63 p.u. fault without FCT is 186.19%, 0.63 p.u. fault with 2.5 cycles FCT is 179.37%, 0.63 p.u. fault with 6.5 cycles FCT is 98.04%, 1.8 p.u. fault with 2.5 cycles FCT is 103.66%, 1.8 p.u. fault with 6.5 cycles FCT is 82.74%, 0.4 p.u. fault without FCT is 231.80%, 0.4 p.u. fault with 2.5 cycles FCT is 178.60%, and 0.4 p.u. fault with 6.5 cycles FCT is 107.88%. This is due to the fact that measurements with a high level of accuracy require longer settling periods than those with a lower level of

accuracy. On the other hand, for the tested system of 1.8 p.u. fault with no-fault clearing time, the implementation of RADR improves transient performance in terms of rising time, settling time (13.51%), peak undershoot, and peak time.

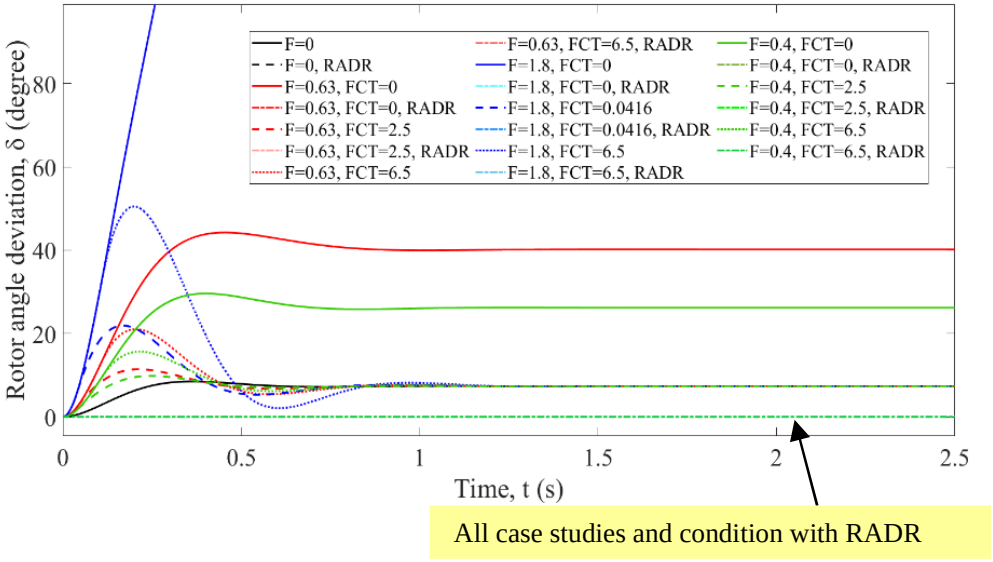

Figure 1. Rotor angle deviation for various fault condition

Table 1. Transient response performance for rotor angle deviation for all cases

Fault (p.u.)	FCT (cycle)	RADR	Rise time (s)	Settling time (s)	Peak time (s)	Peak (δ)
No fault	None	No	0.1495	0.7875	0.3630	8.4898
		Yes	0.3930	2.1305	0.1320	8.79×10^{-5}
0.63	None	No	0.1910	0.7445	0.4545	44.2536
		Yes	0.3885	2.1307	0.1320	8.79×10^{-5}
	2.5	No	0.0495	0.7628	0.2128	11.4164
		Yes	0.3802	2.1310	0.1318	8.79×10^{-5}
	6.5	No	0.0365	1.0762	0.2042	21.0292
		Yes	0.3662	2.1313	0.1320	8.79×10^{-5}
1.8	None	No	1.8175	2.4640	2.5000	2180
		Yes	0.3753	2.1310	0.1317	8.79×10^{-5}
	2.5	No	0.0171	1.0465	0.1685	21.9
		Yes	0.3705	2.1313	0.1320	8.79×10^{-5}
	6.5	No	0.0160	1.1660	0.1995	50.5
		Yes	0.3535	2.1308	0.1318	8.79×10^{-5}
0.4	None	No	0.1672	0.6422	0.4008	29.6
		Yes	0.3878	2.1308	0.1318	8.79×10^{-5}
	2.5	No	0.0811	0.7648	0.2472	9.81
		Yes	0.3488	2.1307	0.1318	8.79×10^{-5}
	6.5	No	0.0472	1.025	0.2155	15.7
		Yes	0.3655	2.1308	0.1318	8.79×10^{-5}

Figure 2 shows the graph of the percentage improvement for peak and peak time for every case. In all cases, the implementation of RADR in the systems results in an optimum percentage improvement of the peak value in the range of 99.9989% to 99.9999%. For the peak time, the systems without FCT recorded a higher percentage of improvement compared to the systems with FCT, which indicates that the implementation of FCT in the system with RADR slowed the peak time of the system.

3.2. Transient response performance for tested system with RADR

The rotor angle deviation graph is shown as indicated in Figure 3 for all cases and conditions when RADR is implemented in the system. It can be seen that the application of RADR yields the same graph regardless of the value of fault and fault clearing time in the system. An underdamped response with a peak undershoots that eventually neared 0° was shown on the rotor angle deviation graph.

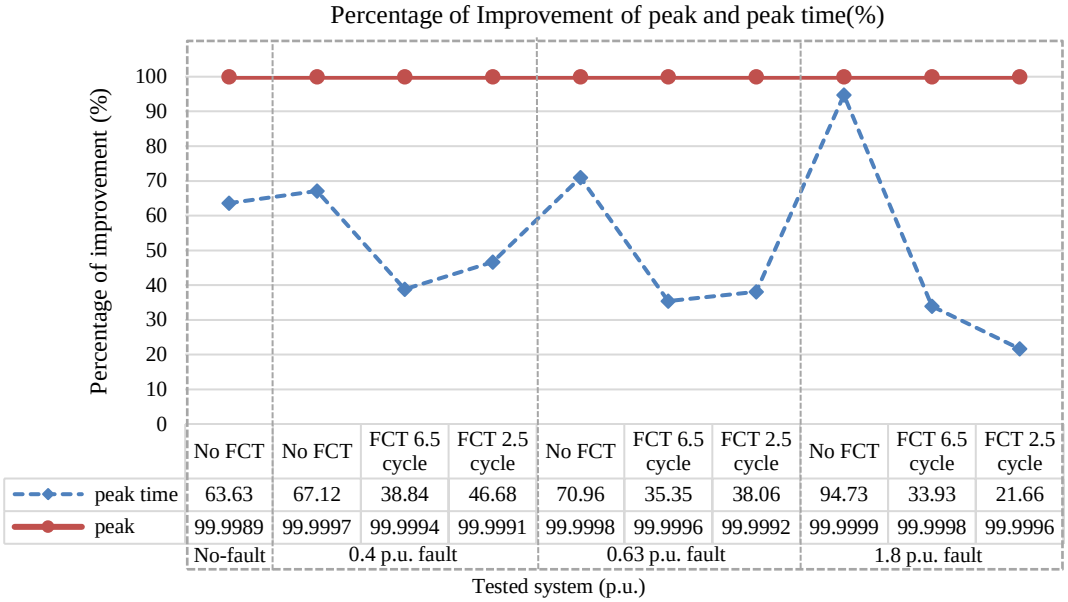

Figure 2. Percentage of improvement of peak and peak time

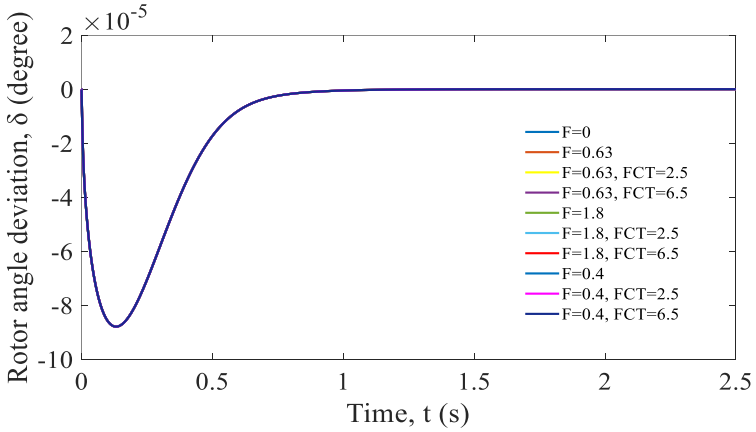

Figure 3. Rotor angle deviation for tested system with RADR

In Figure 4, the final values of rotor angle deviation for all case studies and conditions when RADR is implemented are shown. Figure 3 appears to record the same final value for the rotor angle deviation, but closer inspection reveals small differences between each case study and condition. The purpose of this investigation is to confirm that the RADR is successful in mitigating rotor angle variation in a variety of conditions and case studies.

The rotor angle deviation increased with fault occurrences in the system, as indicated by the blue block. However, it is important to note that for 0.63 p.u. fault occurrences, the recorded rotor angle deviation was less than for the system with 0.4 p.u. fault and no fault. Conversely, when comparing a specific faulty system to its defective system employing FCT, the system with 0.4 p.u. and 0.63 p.u. demonstrates that the faster the fault is eliminated, the higher the reported rotor angle variation. In contrast, the rotor angle deviation of the 1.8 p.u. faulty system decreases as the fault clearance time reduces. In contrast to the faulty system, the 1.8 p.u. faulted system without FCT observed a smaller rotor angle deviation. As a result, the study discovered that increasing fault incidence in the system caused a slight rise in rotor angle deviation. In addition, there is a slight rise in rotor angle deviation following the deployment of FCT in the faulty system, which was expected to help restore system stability. However, the incredibly minimal rotor angle deviation that was observed, irrespective of the case studies and conditions, confirmed that the research objective of regulating the rotor angle deviation to consistently approach 0° had been accomplished.

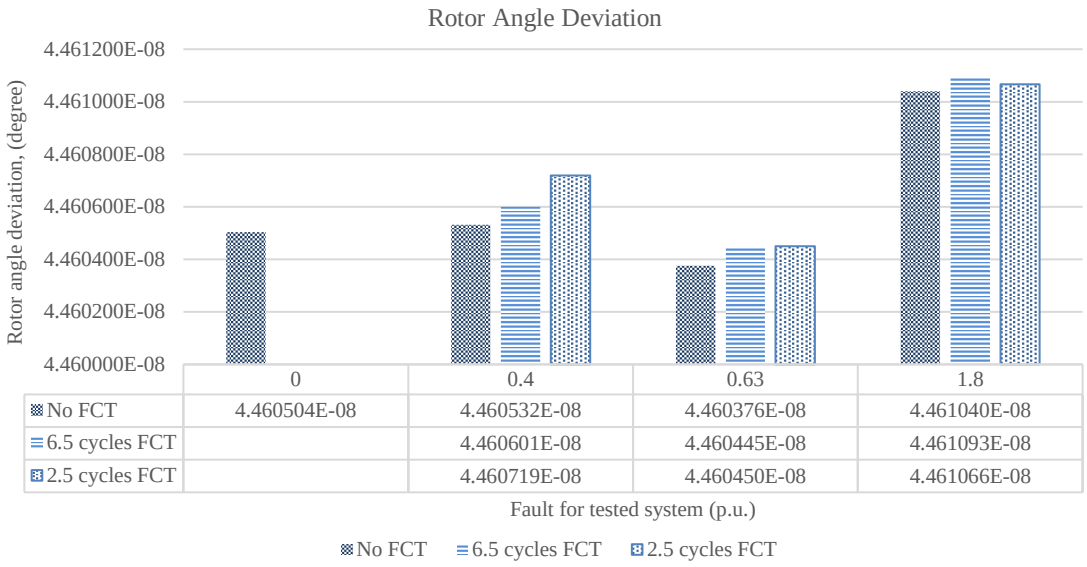

Figure 4. Final value of the rotor angle deviation for the tested system with RADR

3.3. Performance index for tested system with RADR

The performance indices of the various tested systems with RADR are tabulated in Table 2 and compared in this section. For all situations and conditions in the tested system, the IAE and ISE reported the same value. In contrast, there is very little difference in the recorded values for SSE. The fact that the predicted rotor angle deviation is 0° and the observed IAE, ISE, and SSE are all incredibly minor indicates that the RADR's robustness has been met. The result also concludes that the asymptotic stability is preserved as the steady-state behavior obtained from the performances indices for all fault cases are quite promising.

Table 2. Performance index for various tested system with RADR

Case Study	Fault(p.u.)	FCT(s)	IAE	ISE	SSE
1	0	0	$3.14x10^{-5}$	$1.99x10^{-9}$	$3.99x10^{-6}$
2	0.63	0	$3.14x10^{-5}$	$1.99x10^{-9}$	$3.99x10^{-6}$
		2.5	$3.14x10^{-5}$	$1.99x10^{-9}$	$4.07x10^{-6}$
		6.5	$3.14x10^{-5}$	$1.99x10^{-9}$	$4.33x10^{-6}$
3	1.8	0	$3.14x10^{-5}$	$1.99x10^{-9}$	$4.03x10^{-6}$
		2.5	$3.14x10^{-5}$	$1.99x10^{-9}$	$4.09x10^{-6}$
		6.5	$3.14x10^{-5}$	$1.99x10^{-9}$	$4.36x10^{-6}$
4	0.4	0	$3.14x10^{-5}$	$1.99x10^{-9}$	$3.99x10^{-6}$
		2.5	$3.14x10^{-5}$	$1.99x10^{-9}$	$4.45x10^{-6}$
		6.5	$3.14x10^{-5}$	$1.99x10^{-9}$	$4.33x10^{-6}$

4. CONCLUSION

This paper provides a detailed procedure to formulate the algorithm for the rotor angle deviation regulatory system called the RADR. The main focus is to maintain the stability of the synchronous generator in power system generation. The result proves that the proposed RADR guarantees the asymptotic rotor angle stability for the nonlinear swing equation by regulating the rotor angle to consistently approach 0° regardless of the fault and fault clearing time. The robustness of the regulator is also proven by the nonlinear swing equation, which takes damping power into account. The efficacy of the proposed RADR algorithm in various fault conditions guarantee the transient and steady state performance, and hence provides conclusive evidence that the proposed RADR helps in ensuring rotor angle stability as well as power system stability.

ACKNOWLEDGEMENTS

This research was supported by the Ministry of Higher Education (MoHE) through Fundamental Research Grant Scheme (FRGS/1/2021/FKE/F00467). We also acknowledge the Universiti Teknikal Malaysia Melaka (UTeM) for research facilities.

REFERENCES

[1] M. A. Zamee, M. M. Hossain, A. Ahmed, and K. K. Islam, "Automatic generation control in a multi-area conventional and renewable energy based power system using differential evolution algorithm," in *2016 5th International Conference on Informatics, Electronics and Vision (ICIEV)*, Dhaka, Bangladesh, 2016, pp. 262–267, doi: 10.1109/ICIEV.2016.7760007.

[2] Y. Shu and Y. Tang, "Analysis and recommendations for the adaptability of China's power system security and stability relevant standards," *CSEE Journal of Power and Energy Systems*, vol. 3, no. 4, pp. 334–339, 2017, doi: 10.17775/cseejpes.2017.00650.

[3] J. Ritonja and B. Polajžer, "Analysis of synchronous generators' local mode eigenvalues in modern power systems," *Applied Sciences (Switzerland)*, vol. 12, no. 1, 2022, doi: 10.3390/app12010195.

[4] A. Safavizadeh, E. Mostajeran, S. Ebrahimi, and J. Jatskevich, "Investigation of torque-angle characteristics of synchronous generators for transient stability analysis using equal area criterion," in *2022 21st International Symposium INFOTEH-JAHORINA (INFOTEH)*, East Sarajevo, Bosnia and Herzegovina: IEEE, 2022, pp. 16–18, doi: 10.1109/INFOTEH53737.2022.9751312.

[5] R. Jegedeesh Kumar and T. Rammohan, "Enhancement of transient stability in power system with multi-machine using facts device," in *Proceedings of 2020 IEEE International Conference on Advances and Developments in Electrical and Electronics Engineering, ICADEE 2020*, 2020, doi: 10.1109/ICADEE51157.2020.9368921.

[6] J. Luo, F. Teng, and S. Bu, "Stability-constrained power system scheduling: A review," *IEEE Access*, 2020, doi: 10.1109/ACCESS.2020.3042658.

[7] C. Andic, A. Ozturk, and B. Turkay, "Rotor angle stability analysis by using Lyapunov's direct method of a SMIB power system," in *2022 4th Global Power, Energy and Communication Conference (GPECOM)*, Nevsehir, Turkey: IEEE, 2022, pp. 296–300, doi: 10.1109/GPECOM55404.2022.9815562.

[8] M. Rahim, "Methods to improve transient stability of low-inertia synchronous machines," in *2022 75th Annual Conference for Protective Relay Engineers, CPRE 2022*, IEEE, 2022, pp. 1–5, doi: 10.1109/CPRE55809.2022.9776599.

[9] S. K. Khaitan, "THRUST: A Lyapunov exponents based robust stability analysis method for power systems," in *2017 North American Power Symposium (NAPS)*, Morgantown, WV, USA, 2017, pp. 1–6, doi: 10.1109/NAPS.2017.8107395.

[10] M. Gu, K. L. Wong, and L. Meegahapola, "Rotor angle stability analysis of AC/DC hybrid power systems with a VSC- HVDC link," in *2018 IEEE PES Asia-Pacific Power and Energy Engineering Conference (APPEEC)*, Kota Kinabalu, Malaysia, 2018, pp. 565–570, doi: 10.1109/APPEEC.2018.8566249.

[11] H. Amano and A. Yokoyama, "Rotor angle stability analysis using normal form method with high penetrations of renewable energy sources-energy index for multi-swing stability," in *2018 Power Systems Computation Conference (PSCC)*, Dublin, Ireland, 2018, pp. 1–6, doi: 10.23919/PSCC.2018.8442791.

[12] Y. Chen, S. M. Mazhari, C. Y. Chung, S. O. Faried, and B. C. Pal, "Rotor angle stability prediction of power systems with high wind power penetration using a stability index vector," *IEEE Transactions on Power Systems*, vol. 35, no. 6, pp. 4632–4643, 2020, doi: 10.1109/TPWRS.2020.2989725.

[13] K. Peng and A. He, "MLE based rotor angle stability assessment of power system," in *2022 IEEE Asia-Pacific Conference on Image Processing, Electronics and Computers (IPEC)*, Dalian, China, 2022, pp. 1606–1609, doi: 10.1109/IPEC54454.2022.9777620.

[14] M. Shahriyari, H. Khoshkhoo, and J. M. Guerrero, "A novel fast transient stability assessment of power systems using fault-on trajectory," *IEEE Systems Journal*, vol. 16, no. 3, pp. 4334–4344, 2022, doi: 10.1109/JSYST.2022.3148815.

[15] M. Sankar, S. G. Bharathi Dasan, and S. Thamizmani, "Real-time transient stability assessment of post fault scenario in power system by using probabilistic neural network," in *2022 IEEE Delhi Section Conference, DELCON 2022*, IEEE, 2022, doi: 10.1109/DELCON54057.2022.9752930.

[16] M. Y. Borodulin, "Rationale for analyzing inter-machine rotor angles in stability studies of large power systems," in *2020 IEEE/PES Transmission and Distribution Conference and Exposition (T&D)*, IEEE, 2020, pp. 1–5, doi: 10.1109/TD39804.2020.9299889.

[17] K. Charafeddine, Y. Ryzhkova, and Y. Matiunina, "Rotor angle stability of synchronous generator for power grid with wind energy," in *2021 International Conference on Industrial Engineering, Applications and Manufacturing (ICIEAM)*, Sochi, Russia, 2021, pp. 147–151, doi: 10.1109/ICIEAM51226.2021.9446448.

[18] A. K. M. K. Hasan, M. H. Haque, and S. M. Aziz, "Damping rotor angle oscillations using battery energy storage systems," in *2020 IEEE International Conference on Power Electronics, Drives and Energy Systems (PEDES)*, Jaipur, India, 2020, pp. 1–6, doi: 10.1109/PEDES49360.2020.9379433.

[19] M. L. Rahman and A. H. Shatil, "Design and implementation of a synchronous generator with rotor angle stability control for damping interarea oscillations of interconnected power systems via PSS," in *2021 International Conference on Information and Communication Technology for Sustainable Development (ICICT4SD)*, Dhaka, Bangladesh, 2021, pp. 331–335, doi: 10.1109/ICICT4SD50815.2021.9396810.

[20] Y. Kumar, R. N. Mishra, and A. Anwar, "Enhancement of small signal stability of SMIB system using PSS and TCSC," in *2020 International Conference on Power Electronics & IoT Applications in Renewable Energy and its Control (PARC)*, Mathura, India, 2020, pp. 102–106, doi: 10.1109/PARC49193.2020.236566.

[21] H. Jiang and Y. Wang, "Power system transient Sstability enhancement using SMC controller under high wind power penetration scenarios," in *2020 2nd International Conference on Electrical, Control and Instrumentation Engineering (ICECIE)*, Kuala Lumpur, Malaysia: IEEE, 2020, pp. 1–10, doi: 10.1109/ICECIE50279.2020.9309620.

[22] G. Tu, Y. Li, and J. Xiang, "Sliding mode control of energy storage systems for reshaping the accelerating power of synchronous generators," *IEEE Transactions on Power Systems*, vol. 38, no. 2, pp. 1242–1256, 2023, doi: 10.1109/TPWRS.2022.3170703.

[23] P. C. Papageorgiou and A. T. Alexandridis, "Stability and robustness enhancement of SGIB systems via angle estimation-based power controllers," in *The 12th Mediterranean Conference on Power Generation, Transmission, Distribution and Energy Conversion (MEDPOWER 2020)*, online conference, 2020, pp. 491–496, doi: 10.1049/icp.2021.1281.

[24] K. Sunny, A. Sheikh, and S. Wagh, "Dynamic mode decomposition for prediction and enhancement of rotor angle stability," in *2020 7th International Conference on Control, Decision and Information Technologies (CoDIT)*, Prague, Czech Republic, 2020, pp. 160–165, doi: 10.1109/CoDIT49905.2020.9263893.

[25] M. Abubakar, B. Hussain, M. M. Majeed, and D. Ali, "Enhancement of rotor angle stability with superconducting fault current limiter," in *2022 International Conference on Recent Advances in Electrical Engineering & Computer Sciences (RAEE & CS)*, Islamabad, Pakistan: IEEE, 2022, pp. 1–6, doi: 10.1109/RAEECS56511.2022.9954579.

[26] E. Jalalabadi, S. Z. Paylakhi, A. Rahimi-kian, and B. Moshiri, "Integral backstepping Lyapunov redesign control of uncertain nonlinear systems," *IET Control Theory and Applications*, vol. 16, no. 3, pp. 330–339, 2022, doi: 10.1049/cth2.12229.

[27] A. Zaidi and Q. Cheng, "An approximation solution of the swing equation using particle swarm optimization," in *2018 IEEE Conference on Technologies for Sustainability (SusTech)*, Long Beach, CA, USA, 2018, pp. 1–5, doi: 10.1109/SusTech.2018.8671355.

BIOGRAPHIES OF AUTHORS

Nor Syaza Farhana Mohamad Murad received her Bachelor of Electrical Engineering (control, instrumentation, and automation) with Honors from Universiti Teknikal Malaysia Melaka (UTeM) in 2011, and M.Sc. in electrical engineering from Universiti Teknikal Malaysia Melaka (UTeM) in 2018. Currently she is a PhD student in Universiti Teknikal Malaysia Melaka. Her research interests include control system and renewable energy. She can be contacted at email: p012110004@student.utem.edu.my.

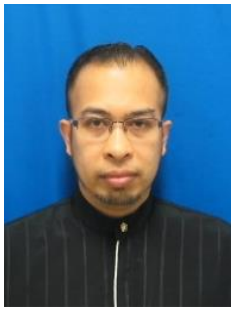

Muhammad Nizam Kamarudin was born in Selangor, Malaysia. He received the B.Eng. (Hons.) electrical from the Universiti Teknologi MARA, Malaysian in 2002, and M.Sc. in automation and control from the University of Newcastle Upon Tyne, United Kingdom in 2007. He received the Doctor of Philosophy in electrical engineering from the Universiti Teknologi Malaysia in 2015. He is currently with the Universiti Teknikal Malaysia Melaka (UTeM). He is the member of the board of engineers, Malaysia and Institute of Engineers, Malaysia. His research interests include nonlinear controls and robust control systems. Before joining UTeM, he worked as a technical engineer at the Magnetron Department of Samsung Electronics Malaysia. He can be contacted at email: nizamkamarudin@utem.edu.my.

Muhammad Iqbal Zakaria is a lecturer at Universiti Teknologi MARA. He obtained his B.Eng. degree in mechatronics from International Islamic University Malaysia in 2010 and his M.Eng. and Ph.D. degrees in electrical engineering from Universiti Teknologi Malaysia in 2012 and 2019 respectively. His research interests include renewable energy, photovoltaic system, and control system. He can be contacted at email: iqbal.z@uitm.edu.my.